

Facile synthesis and characterization of mesoporous titanium oxide nanoparticles for ethanol sensing properties

Altaf Hussain Shar¹, Muhammad Nazim Lakhani¹, Jingyuan Liu¹, Mukhtiar Ahmed¹,
Muhammad Basit Chandio², Ahmer Hussain Shah³, Abdul Hanan¹, Irfan Ali⁴, Jun
Wang¹

Abstract:

Mesoporous TiO₂ nanoparticles were successfully synthesized via solvothermal. The morphology and crystal structure was characterized by UV-vis spectrum (UV-Vis), Fourier Transform Infrared (FTIR) spectroscopy, X-ray diffraction (XRD), Scanning electron microscopy (SEM) and transmission electron microscopy (TEM). All the observations confirmed that the as-fabricated mesoporous TiO₂ nanoparticles were successfully synthesized with surface Plasmon resonance peak between a range of 250-350 nm and its pattern meets with the JCPDS Standard (card No. 21-1272). TEM confirmed the mesoporous structure morphology and shows the incredible gas sensing performance due to their large accessible surface area. Furthermore, the as-prepared TiO₂ nanoparticles exhibited more rapid response/recovery and higher sensitivity towards ethanol at 180°C distinguished with isopropyl alcohol and methanol. In addition, it can be affirmed that the synthesized mesoporous TiO₂ nanoparticles are a promising applicant for fabricating high-performance ethanol gas sensor in real-time monitoring.

Keywords: Gas sensor; mesoporous; nanotechnology; TiO₂; ethanol sensing.

1. Introduction

Currently, atmospheric environmental protection is considered as a concerning issue because of the emission of harmful gas molecules and due to the rapid development in modern industries. To mitigate this, the

detection of toxic gases is extremely essential for the excellence of the environment and human health [1]. Vapor sensors based on ethanol are widely usable sensors owing to their unique properties in chemical and biomedical industries and also for the analysis of breath [2]. High sensitivity, minimum

¹Key Laboratory of Superlight Material and Surface Technology, Ministry of Education, Harbin Engineering University, PR People's Republic of China.

²College of Mechanical and Electrical Engineering, Harbin Engineering University, People's Republic of China

³Department of Textile Engineering, Balochistan University of Information Technology, Engineering and Management Sciences, Quetta, Pakistan

⁴College of Chemical Engineering, Beijing University of Chemical Technology, People's Republic of China

Corresponding Author: altafshar12@gmail.com

operating temperature, and less recovery time with short responses are ideal features in ethanol vapor (EV) sensors. Therefore, EV sensors and their functional materials research attracted huge attention by scientists for the development of high-performance EV sensors.

Nowadays, many sensing mechanisms and technologies have been employed for volatile organic compounds (VOCs) detection including thermal conductivity, catalyst, electrochemical, chemi-resistors types, mechanical and optical [3]. Among them, chemi-resistors based sensors are mostly preferable and economical devices with the existence of transducing platforms and acceptor materials and are broadly accepted because of their high potential application and long-term stability [4].

The gas sensing material is considered an important parameter for the selection of gas sensors. Among many, metal oxide semiconductors (MOSs) nanomaterials have attained some significant attention and considered promising material due to advantages such as; easy fabrication, fast response and recovery time, low operating cost, minimum power consumption, and minimum size with excellent chemical stability [5]. Mesoporous semiconducting metal oxides have been extensively used as the chemi-resistive based gas sensors due to their outstanding properties such as high surface area, large pores volume, high interconnection, long-term stability, high electron conductivity and enhanced sensing performance [6]. Among other metal oxides, Titanium dioxide (TiO_2) with wide-bandgap (3.4 eV) MOSs are considered as promising material Because of its distinctive properties includes chemical stability, excellent sensor performance, low cost, high activity, non-toxicity and abundance [7], and is used in various applications including batteries [8], photocatalysis, water splitting, solar cells, gas sensors, and biological application [9]. TiO_2

attracts much attention in the field of gas sensors [10]. In comparison with some common MOSs gas sensors operated on high temperatures, TiO_2 is favorable owing to higher sensitivity, fast response, long-term stability, and easily detectable gas at low temperatures. Various structures of TiO_2 used for ethanol detection have been reported, such as nanoparticles and nanoflowers [11, 12]. However, pristine TiO_2 is not widely investigated due to they are some drawbacks including low sensitivity, slow response-recovery time and limited specific area [13]. To solve these problems, many researchers committed to enhance the performance of TiO_2 based sensors to modify morphology of TiO_2 surface and nanostructure, as they are key factors that influence gas sensing performance [14]. Particularly, mesoporous TiO_2 nanostructures have a large specific surface area which provides numerous active sites facilitating more oxygen to be adsorbed at the surface and it also allows gas molecules to easily penetrate and adsorb on the surface of sensing materials for the improvement of response recovery time and detection limit [15]. Much research has still to be made for the development of mesoporous sensing materials having properties such as high sensitivity, minimum operating temperature, short response with less recovery time, easy fabrication and environmental flexibility.

Herein, a novel ethanol vapor based sensor on mesoporous TiO_2 nanoparticles has been successfully synthesized via solvothermal methods. The as-fabricated mesoporous TiO_2 material microstructure properties were characterized by FTIR, UV-Vis, XRD, SEM and TEM. Furthermore, Gas sensing properties such as operating temperature, response to concentration, selectivity, response and recovery time were evaluated.

2. Materials and method

2.1. Synthesis mesoporous TiO₂ nanoparticles:

All the chemicals we used in this experiment are of analytical grade and used directly without any further purification prior to usage. Mesoporous TiO₂ nanoparticles are prepared by an environmentally friendly and one-step Solvothermal route. In a typical process, first 20 ml of deionized water (DW) and 40ml isopropyl alcohol were mixed together using magnetic stirrer until a homogeneous solution formed. Then, 6.0 g of titanium sulfate (Ti (SO₄)₂) was added under strong stirring till a uniform solution achieved. Afterward, the aqueous solution was transferred into 100 ml Teflon-lined stainless steel autoclave and heated at 90°C for 12 h. Later, as-prepared TiO₂ were centrifuged, rinsed and overnight dried at 90°C. Finally, the dried powder was calcined in tube furnace at 300°C for 2 h in atmospheric air at a rate of 5 °C/min.

2.2. Characterization

UV-Vis absorption spectra were calculated by using a TU-1901 dual-beam UV-Vis spectrophotometer. The FTIR spectrum of mesoporous nanoparticles was collected on KBr plates cast using a Perkin Elmer Spectrum 100 FTIR spectrometer. The crystal structure was investigated by XRD system with Cu K1 radiation ($\lambda = 0.15406$ nm). The surface morphology of catalyst was observed with SEM (JOEL JSM – 6480A) operated at a 20kv of driving voltage while TEM images were acquired by using an FEI TECNNI G2 instrument. The gas sensing measurements were tested by a commercial NMDOG multi-functional accuracy sensor analysis tester (manufactured in Changsha city, China) at room temperature.

2.3. Fabrication and measurement of the sensor

In a typical process, the as-prepared sensing material was fully grinded by adding a small amount of ethanol to form slurry, and then pasted it onto the ceramic tube and then heated at 60°C for 2 h to evaporate the ethanol and kept in air for one day to improve the stability of the sensing materials layer. The operating temperature was controlled by providing the heating current through the Ni-Cr, resistor heating wire inserted into the ceramic tube. Sensing properties of the gas sensor were measured by a commercial NMDOG Multifunctional Precision Sensor Analysis Instrument (Changsha Dingchen Scientific Instrument Co, Ltd, Hunan, China). For measurement, the saturated target vapor in corresponding amounts was injected into a closed 10 L chamber by a micro-syringe to obtain the different concentrations of analytes. After fully mixed with atmospheric air, the sensor was put into the chamber to measure its performance. When the response on the display reached constant value, the sensor was taken out to atmospheric air. The response of the sensor is defined as the $S=R_g/R_a$, where R_g is the resistance of the sensor in target gas and R_a is the resistance of the sensor in air.

The response/ recovery time is defined as time spent by the sensor to achieve 90% of the total resistance change.

3. Results and Discussion

3.1. UV-Visible spectrum

The UV-Vis absorption spectrum of mesoporous TiO₂ nanoparticles is shown in Fig. 1. UV-Vis spectrum of TiO₂ sharp edge 250-350 nm showing mesoporous TiO₂ nanoparticles absorbs light from the ultraviolet region at room temperature displaying a good absorption band in the UV region [16].

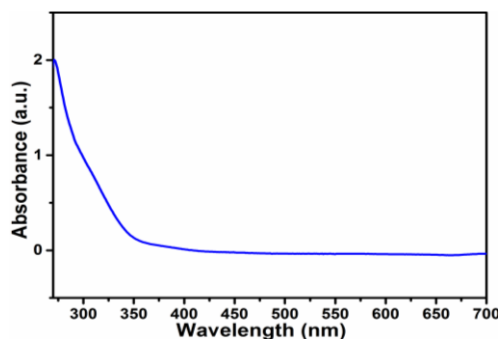


Fig 1. The UV-Visible spectrum of mesoporous titanium dioxide nanoparticles.

3.2. FTIR analysis

FTIR spectroscopy was used to characterize the proper surface functional groups responsible for the synthesis of mesoporous TiO₂ nanoparticles as shown in Fig. 2. The intensive absorption peaks were characterized by a number of characteristic bands occurring at 3744 cm⁻¹, 3648 cm⁻¹, 2917 cm⁻¹, 2853 cm⁻¹, 1741 cm⁻¹, 1585 cm⁻¹, 1376 cm⁻¹ and 1118 cm⁻¹. The characteristic peaks were noticed between 3700 cm⁻¹ and 3500 cm⁻¹ were related to TiO₂ product as well as small intensity peak at 1650 cm⁻¹ was showing stretching and bending vibrations of hydroxyl groups on the surface of TiO₂ nanoparticles. Additionally, another absorption peaks situated at 2917 and 2853 cm⁻¹ were assigned to the asymmetric and symmetric stretch vibrations of CH₂ groups, 1740 cm⁻¹ represents the stretching of C=O aldehydes group, 1586 cm⁻¹ (C-C) stretches in the aromatic ring, 1420 cm⁻¹ (CH groups) and 1118 cm⁻¹ (C=O stretching vibrations). The obtained peaks in spectra confirm the formation of final TiO₂ products [17].

3.3. XRD analysis

XRD pattern confirms the composition and crystal structure of as-synthesized TiO₂ nanoparticles. Materials were characterized in a range of 10-90. Fig. 3 depicted the XRD patterns of the obtained anatase TiO₂ sample. All the diffraction peaks located at 2θ = 25.2, 37.8, 48.0, 53.9, 55.0, 62.7, 68.7, 70.3 and 75.0 could be indexed to (101), (004), (200),

(105), (211), (204), (116), (220) and (215) planes of anatase TiO₂, respectively. The peaks of the anatase TiO₂ phase are of (JCPDS card No. 21-1272) standard. No characteristic peaks of impurity phases were observed in the XRD pattern and sharp diffraction peaks indicated good crystallinity. The grain size of mesoporous TiO₂ nanoparticles was calculated using the Scherrer formula [18].

$$D = (k\lambda) / (\beta \cos\theta)$$

Where D is average crystallite size, λ is the wavelength of Cu Kα (0.154 nm), k is a shape factor which is 0.9, β is measured from the full width at half maximum (FWHM) in radian and θ is Bragg angle it is obtained by dividing 2 the 2θ value of corresponding diffraction peak. The mean crystallite sizes of mesoporous TiO₂ nanoparticles were found in the ranges of 17-24 nm as shown in table 1.

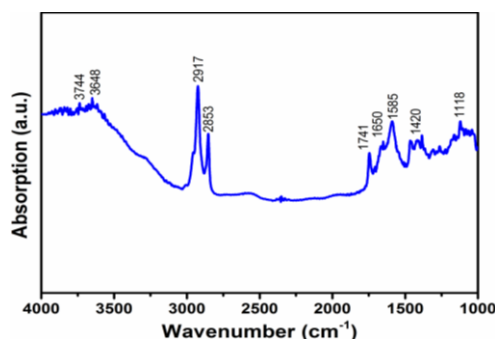


Fig 2. FTIR analysis of mesoporous TiO₂ nanoparticles.

Table 1. Particle size calculation from the XRD pattern.

| Lattice plane | Peak Position (degree) | FWHM (degree) | Particle size (nm) |
|---------------|------------------------|---------------|--------------------|
| (101) | 25.2 | 0.47 | 17.3 |
| (004) | 37.8 | 0.57 | 17.8 |
| (200) | 48.0 | 0.40 | 18.4 |
| (211) | 55.0 | 0.37 | 19.0 |
| (215) | 75.0 | 0.20 | 48.5 |

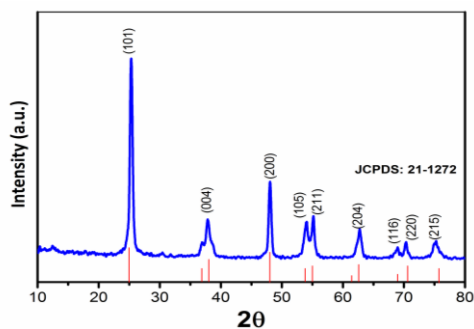


Fig 3. XRD patterns of mesoporous TiO₂ nanoparticles

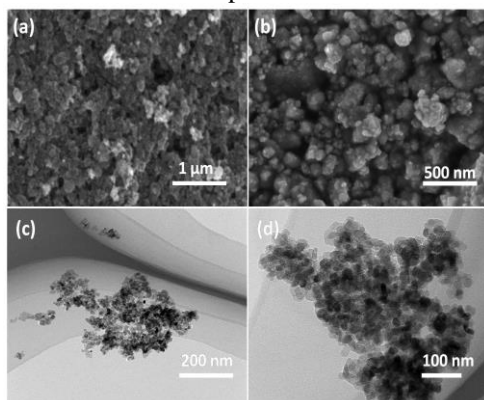


Fig 4. (a-b) SEM images of mesoporous TiO₂ nanoparticles and TEM (c-d).

3.4. Morphology and structure analysis

The morphology of the as-synthesized mesoporous TiO₂ nanoparticles sample was investigated by SEM. Fig. 4a depicted that as-obtained mesoporous TiO₂ nanoparticles were adhered to by many small size mesoporous particles that are densely distributed inside and outside of the substrate surface. Fig. 4b showed that the fine nanoparticles are assembled on the mesoporous surface of TiO₂ pores were agglomerated to form large particles (lumps) and the shape of nanoparticles is irregular with their average sizes range around 20-200 nm.

The microstructure of mesoporous TiO₂ nanoparticles was further investigated by the TEM technique. Fig. 4c revealed that the

higher degree of mesoporous structure and also large number of pores appeared on the surface of the as-prepared mesoporous TiO₂ nanoparticles. Fig. 4d showed the HRTEM images of mesoporous TiO₂ nanoparticles from there we could be observed that the shape of particles is irregular and their average size ranges 20-70 nm. TEM results are correlated with SEM results.

3.5. Gas Sensing Properties

The porous structure plays a vital role in determining the sensing properties by affecting the diffusion of test gases toward sensing material surface [19]. The operating temperature of the sensor is significantly influenced by MOSs based sensors. Therefore, the gas sensing performance of the mesoporous TiO₂ nanoparticles to 100 ppm ethanol gas was examined. Fig. 5a revealed the response of the sensor toward 100 ppm ethanol at an operating temperature from 100°C to 220°C. it is found that the response increased with the initial operating temperature, and reached the maximum value at about 180 °C, afterward the response decreased with further increment in temperature then the existence of an optimal temperature was observed, which is finally taken as 180°C with the strongest response value of the sensor based on TiO₂ is 5.2 at 180 °C. The selectivity is a crucial parameter for the gas sensor to evaluate the sensing performances of gas sensors for their practical application. Thus, the selectivity test of the sensor was investigated by exposing several kinds of common gases including ethanol, isopropyl alcohol, and methanol tested with a concentration of 100 ppm at the same temperature of 180 °C and the results are shown in a bar graph as shown in Fig. 5b. Clearly, it can be observed that the sensor-based mesoporous TiO₂ nanoparticles exhibited a much higher response to ethanol in comparison to any other gases at the same concentration. The response and recovery time also plays a significant role in the

practical detection of detrimental gases. Fig. 6 showed a dynamic curve of mesoporous TiO₂ nanoparticles response and recovery towards 100 ppm ethanol gas at 180°C was plotted. The result affirms that the resistance of the sensor instantly changes when the sensor was exposed to targeted gases, and later reached a steady state. The response and recovery time of the sensor to ethanol was within 25 s and the recovery time was 15 s, respectively.

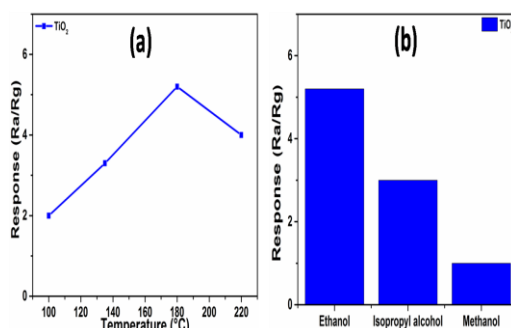


Fig 5. (a) Response of the different mesoporous TiO₂ nanoparticles versus operating temperature to 100 ppm acetone (b) Selectivity of mesoporous TiO₂ nanoparticles towards 100 ppm of various gases.

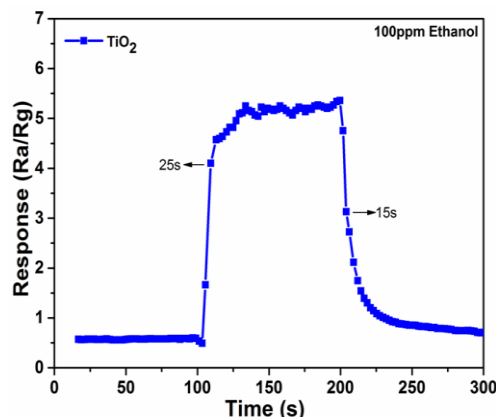


Fig 6. The response-recovery dynamic curve of mesoporous TiO₂ nanoparticles to 100 ppm ethanol at 180°C.

4. Conclusion

We have successfully prepared mesoporous TiO₂ nanoparticles by a simple and low cost solvo thermal method under the calcinations temperature at 300°C. The as-obtained sample was characterized by various analytic techniques and their gas sensing properties were examined. It is found that the mesoporous structure of TiO₂ nanoparticles exhibits high surface area and large pore volume and showed a better performance of ethanol sensing towards 100 ppm at 180°C with fast response and recovery times. The enhancements of gas sensing properties were ascribed to the distinctive porous structure.

ACKNOWLEDGMENT

The author thanks the financial support of the National Natural Science Foundation of China (NSFC 51402065 and 51603053), Natural Science Foundation of Heilongjiang Province (B2015021), Fundamental Research Funds of the Central University, the Application Technology Research and Development Projects of Harbin (2015RAQXJ038) and Defense Industrial Technology Development Program (JCKY2016604C006).

References

- [1]. N. T.A.Thu, N.D. Cuong, L.C. Nguyen, D.Q. Khieu, P.C. Nam, N.V. Toan, C.M. Hung, N.V. Hieu, Fe₂O₃ nanoporous network fabricated from Fe₃O₄/reduced graphene oxide for high-performance ethanol gas sensor, *Sensors and Actuators B: Chemical*, Vol. 255, 2018, pp. 3275-3283.
- [2]. D.R. Miller, S.A. Akbar, P.A. Morris, Nanoscale metal oxide-based heterojunctions for gas sensing: A review, *Sensors, and Actuators B: Chemical*, Vol, 204, 2014, pp. 250-272.
- [3]. T. Yuan, Z. Li, W. Zhang, Z. Xue, X. Wang, Z. Ma, Y. Fan, J. Xu, Y. Wu, Highly sensitive ethanol gas sensor based on ultrathin nanosheets assembled

- Bi₂WO₆ with composite phase, Science Bulletin, Vol. 64, 2019, pp. 595-602.
- [4]. M. Tonezzer, L.T.T. Dang, H.Q. Tran, S. Iannotta, Multiselective visual gas sensor using nickel oxide nanowires as chemiresistor, Sensors, and Actuators B: Chemical, Vol. 255, 2018.
- [5]. A. Dey, Semiconductor metal oxide gas sensors: A review, Materials Science and Engineering: B, Vol. 229, 2018, pp. 206-217.
- [6]. N.D. Hoa, S.A. El-Safty, Highly sensitive and selective volatile organic compound gas sensors based on mesoporous nanocomposite monoliths, Analytical Methods, Vol. 3, 2011, pp. 1948-1956.
- [7]. R. Wilson, C. Simion, C. Blackman, C. Carmalt, A. Stanoiu, F. Di Maggio, J. Covington, The Effect of Film Thickness on the Gas Sensing Properties of Ultra-Thin TiO₂ Films Deposited by Atomic Layer Deposition, Sensors, Vol. 18, 2018, pp. 735.
- [8]. M.V. Reddy, G.V. Subba Rao, B.V.R. Chowdari, Metal Oxides and Oxysalts as Anode Materials for Li Ion Batteries, Chemical Reviews, Vol. 113, 2013.
- [9]. A. Bertuna, E. Comini, N. Poli, D. Zappa, G. Sberveglieri, Titanium Dioxide Nanostructures Chemical Sensor, Procedia Engineering, Vol. 168, 2016, pp. 313-316.
- [10]. C. Wang, Y. Li, P. Qiu, L. Duan, W. Bi, Y. Chen, D. Guo, Y. Liu, W. Luo, Y. Deng, Controllable synthesis of highly crystallized mesoporous TiO₂/WO₃ heterojunctions for acetone gas sensing, Chinese Chemical Letters, (2019).
- [11]. S. Nasirian, H. Milani Moghaddam, Hydrogen gas sensing based on polyaniline/anatase titania nanocomposite, International Journal of Hydrogen Energy, Vol. 39, 2014, pp. 630-642.
- [12]. A. H. Shar, M. N. Lakhan, J. Wang, M. Ahmed, K. T. Alali, R. Ahmed, I. Ali, A. Q. Dayo, facile synthesis and characterization of selenium nanoparticles by the hydrothermal approach, Digest Journal of Nanomaterials and Biostructures, Vol. 14, 2019, pp. 867-872.
- [13]. J. Zhang, X. Liu, G. Neri, N. Pinna, Nanostructured Materials for Room-Temperature Gas Sensors, Advanced Materials, Vol. 28, 2016, pp. 795-831.
- [14]. S. Zhang, P. Song, Z. Yang, Q. Wang, Facile hydrothermal synthesis of mesoporous In₂O₃ nanoparticles with superior formaldehyde-sensing properties, Physica E: Low-dimensional Systems and Nanostructures, Vol. 97, 2018, pp. 38-44.
- [15]. S. Liu, Z. Wang, H. Zhao, T. Fei, T. Zhang, Ordered mesoporous Co₃O₄ for high-performance toluene sensing, Sensors and Actuators B: Chemical, Vol. 197, 2014, pp. 342-349.
- [16]. B. Durairaj, T. Xavier, S. Muthu, fungal generated titanium dioxide nanopartilces for uv protective and bacterial resistant fabrication, International Journal of Engineering Science and Technology (IJEST), Vol. 6, 2014, pp. 621-625.
- [17]. G. Rajakumar, A. A. Rahuman, S. M. Roopan, V. G. Khanna, G. Elango, C. Kamaraj, A. A. Zahir, K. Velayutham, Fungus-mediated biosynthesis and characterization of TiO₂ nanoparticles and their activity against pathogenic bacteria, Spectrochim Acta A Mol Biomol Spectrosc, Vol. 91, 2012,
- [18]. F. T. L. Muniz, M. A. R. Miranda, C. M. D. Santos, J. M. Sasaki, The Scherrer equation and the dynamical theory of X-ray diffraction, Vol. 72, 2016, pp. 1-6.
- [19]. Z. Wen, L. Zhu, Y. Li, Z. Zhang, Z. Ye, Mesoporous Co₃O₄ nanoneedle arrays for high-performance gas sensor, Sensors and Actuators B: Chemical, Vol. 203, 2014, pp. 873-879.